Journal of Physics:
Conference Series

PAPER • **OPEN ACCESS**

One-year dynamic monitoring of a steel-concrete composite overpass

To cite this article: Carmelo Gentile and Marco Pirrò 2024 *J. Phys.: Conf. Ser.* **2647** 042004

Journal of Physics: Conference Series **2647** (2024) 042004 doi:10.1088/1742-6596/2647/4/042004

One-year dynamic monitoring of a steel-concrete composite overpass

Carmelo Gentile and Marco Pirrò

Department of Architecture, Built environment and Construction engineering, Politecnico di Milano, P.za Leonardo da Vinci 32, 20133 Milan - Italy

carmelo.gentile@polimi.it

Abstract. Selected results collected in the continuous dynamic monitoring of a 3-span overpass using MEMS accelerometers are reported in the paper. The investigated structure is a steel-concrete composite bridge with a trapezoidal box girder of variable height and curved cross-beams, so that the overall geometry is rather complex. The overpass has a total length of 108 m and spans of 30 m + 48 m + 30 m. The paper firstly presents the dynamic characteristics of the structure obtained from preliminary ambient vibration tests. Subsequently, the effects of environmental and operational variability during the continuous monitoring are highlighted, with the temperature significantly affecting all natural frequencies. A clear effect of changing environment is detected for torsion modes as well, whereas no remarkable changes of bending mode shapes are observed.

1. Introduction

A fundamental issue in the management of transportation networks relies with the bridges approaching the end of their design lifetime. In addition, the deterioration rate of bridges tends to increase with increased service loads (traffic), progressive degradation of materials caused by aging as well as with deferred or poor maintenance (see e.g., [1]).

Within this context, vibration-based Structural Health Monitoring (SHM) has received increasing attention and the installation of dynamic monitoring systems on bridges has become more common [2] in the last few years. Well-known examples of permanently instrumented bridges in different countries include the Z24 bridge [3] in Switzerland, the Infante D. Enrique bridge [4] in Portugal, the Tamar bridge [5] in South-west England, the San Michele bridge [6] and the Brivio bridge [7] in Italy.

A satisfactory identification of the occurrence of structural anomalies can be performed by applying the Statistical Pattern Recognition (SPR) [8] paradigm to continuously identified modal parameters [4]: since especially the natural frequencies are strongly affected by environmental and operational variability [3], the main objective of the SPR approach is to distinguish patterns related to the normal structural conditions under operational and environmental variability from those associated with the onset of structural anomalies or damaged conditions. To this purpose, both supervised and unsupervised regression models [9] are generally applied to filter out the normal changes of automatically identified modal parameters during a training period; subsequently, SPR is adopted to assess the presence of changes in the healthy state of the investigated structure through control charts (such as the one based on T^2-statistic [10]).

The present paper is mainly aimed at presenting selected results from the dynamic monitoring of a steel-composite overpass. After a concise description of the bridge and the monitoring system, details are given on the software tools employed to process the continuously acquired data. Subsequently, the dynamic characteristics of the overpass, that were identified in preliminary tests (and verified during the first hours of continuous monitoring), are presented and discussed. The last part of the paper focuses on the results of the monitoring for a period of 1 year and special attention is paid to the influence of environmental parameters on the variations observed in both resonant frequencies and (torsion) mode shapes.

2. The *Dolo* overpass

The *Dolo* Overpass (figure 1a) is a steel-composite bridge that crosses the A4 Milan-Venice highway in the municipality of Dolo (VE). The infrastructure has an overall length of 108 m (figures 1 and 2) and consists of three spans of different lengths: the largest span, crossing the A4, is 48 m long whereas the length of side-spans is 30 m. The continuous deck − housing a roadway of 12 m and two walkways of 1.7 m each – consists of a trapezoidal steel box girder that is composite with a r.c. slab and stiffened by equally spaced steel cross-beams (figure 1b).

As shown in figure 1, the central span is supported by elastic constraints made of inclined steel struts resting on squat r.c. piers.

a)

b)

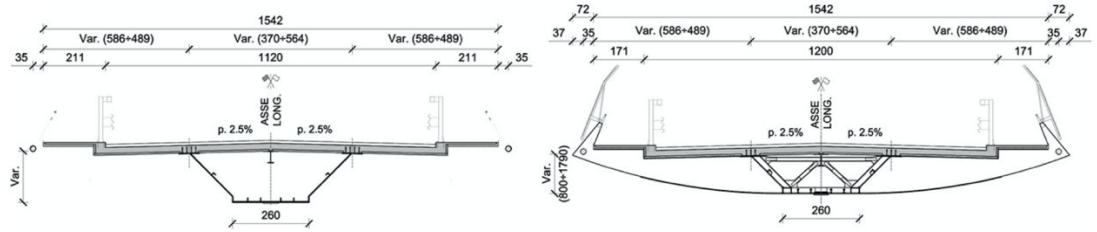

Figure 1. View (a) and transversal cross-sections (b) of the *Dolo* overpass (dimensions in cm).

3. Automated modal identification and reference vibrations modes

After preliminary ambient vibration test (AVTs), performed in November 2020, a dynamic monitoring system has been installed on the bridge. The monitoring system is fully active since the second half of January 2022 and includes 22 MEMS accelerometers (1 V/g sensitivity, ± 2g peak acceleration, 22.5 μg/√Hz noise density and 24-bit resolution) and one temperature sensor to evaluate the correlation between the air temperature and the automatically identified modal parameters (figure 2).

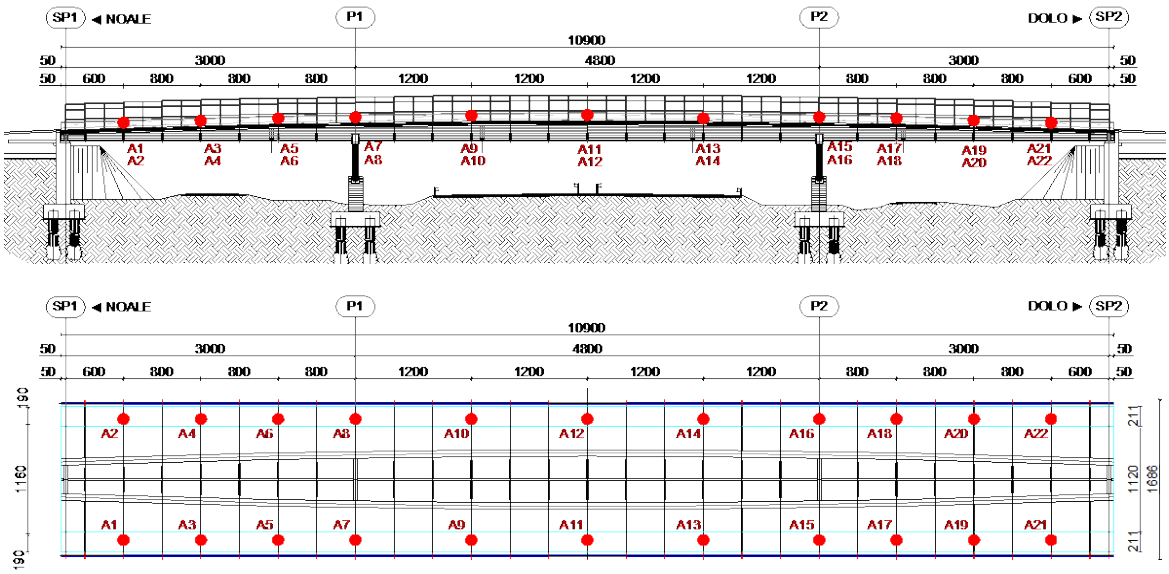

Figure 2. Elevation and plan of the *Dolo* overpass (dimensions in cm) and scheme of the monitoring system.

In the first year of monitoring (from 23 January 2022 to 22 January 2023), 8760 datasets have been collected and processed: the modal parameters are automatically identified using MATLAB software package called DYMOND [11] and based on the covariance-driven Stochastic Subspace Identification (SSI-Cov) algorithm [12]. SSI procedures [12] are based on the discrete-time stochastic state-space form of the dynamics of a linear-time-invariant system under unknown excitation:

$$\boldsymbol{x}_{k+1} = \boldsymbol{A} \cdot \boldsymbol{x}_k + \boldsymbol{w}_k \tag{1}$$

$$\boldsymbol{y}_{k+1} = \boldsymbol{C} \cdot \boldsymbol{y}_k + \boldsymbol{v}_k \tag{2}$$

where $\boldsymbol{x}_k \in \Re^n$ is the discrete-time state vector (containing displacements and velocities at time step k), $\boldsymbol{y}_k \in \Re^m$ is the vector collecting the m output measurements, $\boldsymbol{A} \in \Re^{n \times n}$ is the system matrix of order n (containing the modal information of the structure), $\boldsymbol{C} \in \Re^{m \times n}$ is the output matrix (mapping the state vector into the measured outputs), $\boldsymbol{w}_k$ and is the process noise and $\boldsymbol{v}_k$ is the measurement noise.

For a selected model order n, the SSI-Cov algorithm estimates the model matrices $\boldsymbol{A}$ and $\boldsymbol{C}$ by using the covariance matrix of the available measurements; subsequently the modal parameters (i.e. natural frequencies, damping ratios and mode shapes) can be computed from the following:

$$\boldsymbol{A} = \boldsymbol{\Psi} \cdot \boldsymbol{\Lambda} \cdot \boldsymbol{\Psi}^{-1} \quad \text{where,} \quad \boldsymbol{\Lambda} = diag(\lambda_i) \quad i = 1, ..., n \tag{3}$$

$$\lambda_i^c = \frac{\ln \lambda_i}{\Delta t} \quad i = 1, \ ..., \ n \tag{4}$$

$$f_i = \frac{|\lambda_i^c|}{2\pi} \quad i = 1, \ ..., \ n \tag{5}$$

$$\xi_i = \frac{\text{real}(\lambda_i^c)}{|\lambda_i^c|} \quad i = 1, \ ..., \ n \tag{6}$$

$$\boldsymbol{\Phi} = \boldsymbol{C} \cdot \boldsymbol{\Psi} \quad \text{where,} \quad \boldsymbol{\Phi} = [\phi_1, \phi_2, ..., \phi_n] \tag{7}$$

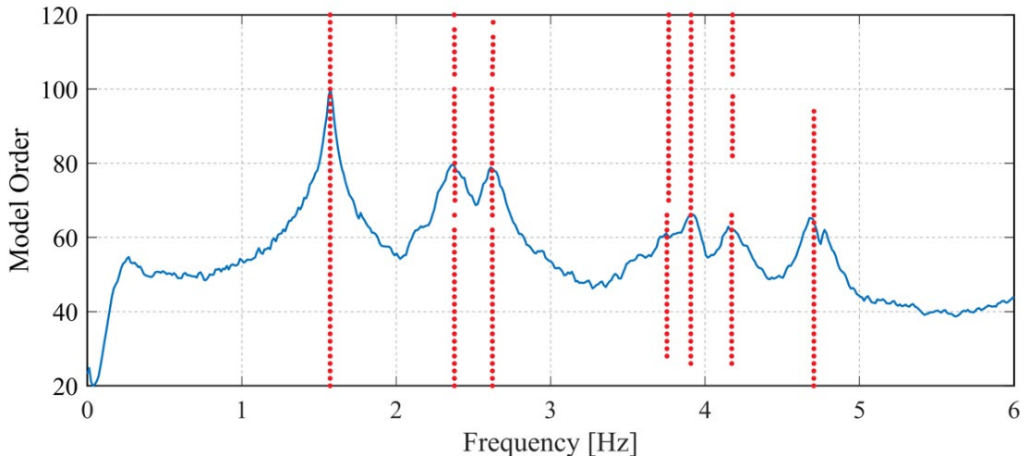

Figure 3. *Dolo* overpass: stabilization diagram (SSI-Cov) obtained from data collected in the AVT of November 2020.

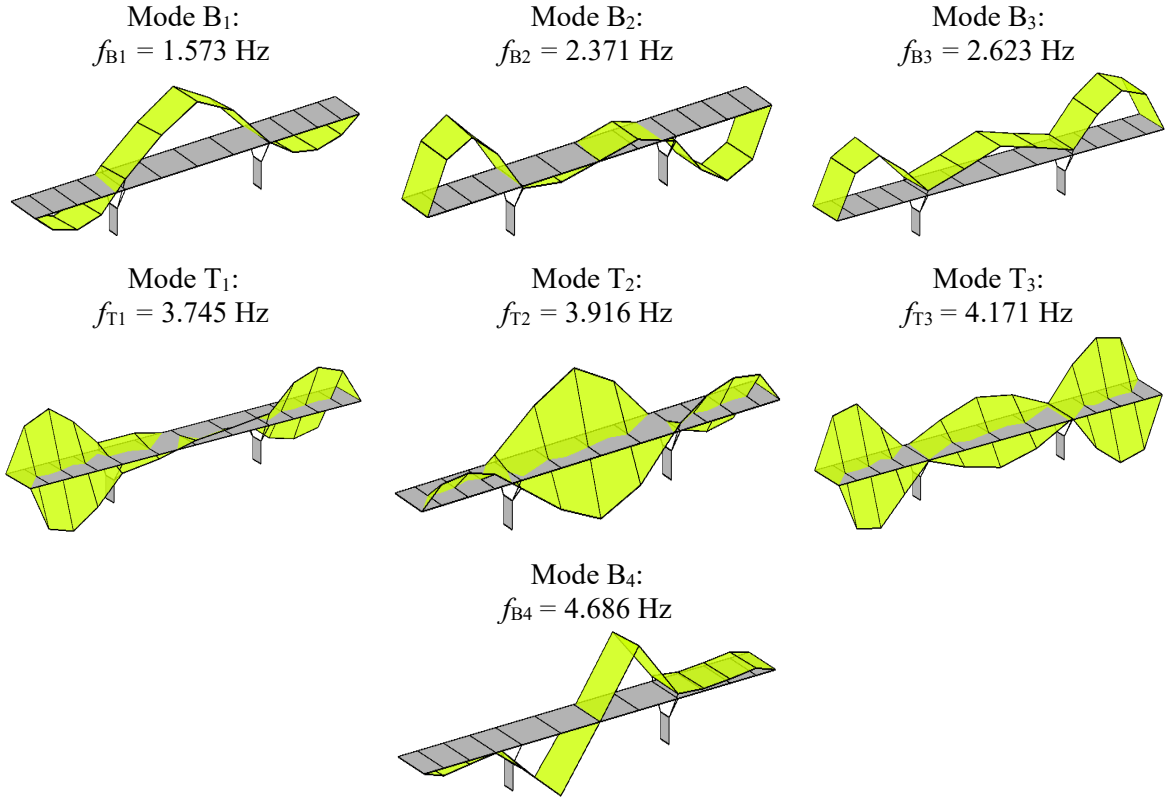

Figure 4. *Dolo* overpass: *reference* mode shapes identified from data collected in the AVT of November 2020.

In practical applications, due to disturbances contained in the responses and to the finite number of samples, the identification of system matrices is carried out for increasing model order n and each set of extracted modal parameters is represented in a stabilization diagram (figure 3). The stabilization diagram allows the visualization of stable alignments composed by physical poles of the state matrix $\boldsymbol{A}$ that maintain a certain degree of consistency for increasing model order.

As previously stated, preliminary AVTs were performed on 10-11 November 2022 using the same sensors layout subsequently adopted in the continuous monitoring (figure 2). During these tests, 7 vibration modes were identified in the frequency range of 0-6 Hz (figure 3); as shown in figure 4, the observed modes can be basically arranged as vertical bending modes (B) and vertical torsion (T) modes of the deck. The identified vibration modes have been also confirmed by the analysis carried out on the first datasets collected during the continuous monitoring.

4. Continuous dynamic monitoring and results

In order to handle with a large number of datasets, the modal tracking procedure illustrated in [13] has been adopted: the procedure automatically collects all the identified modes from each dataset, tracking only the ones that share similar modal characteristics with the *reference* modes (figure 4). In more details, the procedure associates the *j-th* mode identified from the *h-th* dataset to the *i-th reference* mode if the deviation in terms of natural frequency and Modal Assurance Criterion (MAC) [14] does not exceed pre-selected thresholds:

$$d_{h,i}^{f} = |f_{h,j} - f_i| < d_{i,max}^{f} \tag{8}$$

$$d_{h,i}^{MAC} = 1 - MAC(\phi_{h,j}, \phi_i) < d_{i,max}^{MAC} \tag{9}$$

After the application of tracking procedure, it is necessary to understand and minimize the effects of environmental (temperature) and operational (traffic) variability on the natural frequencies [3]-[7]. In the present case, a PCA model [9] is defined over a training period of appropriate length (in which it is assumed that the structure maintains its normal condition) to account for the "mask effects" arising from environmental and operational changes. The PCA is a multi-variate technique that finds the variability common to various time-series (in this context the time series are represented by the identified natural frequencies): once the PCA regression model has been defined on a training period, in such a way to find the variability mainly due to environmental and operational effects, the model is used to reconstruct the time series and the residuals between identified and predicted time series conceivably contains only the effects of possible structural variations. Consequently, the residuals can be used to detect structural anomaly occurrences by adopting multi-variate control-charts, such as the one based on Hotelling T^2-statistic [10], [4].

4.1. Results

Figure 5 shows the time variation of the automatically identified frequencies of the investigated overpass during the first weeks of monitoring (i.e., from 23 January 2022 to 24 March 2022) and clearly suggests that the evolution of natural frequencies exhibits a daily pattern, conceivably due to temperature variation. In addition, the influence of temperature is clearly detected in figure 6 − illustrating the time evolution of the identified frequencies (figure 6a) and the measured air temperature (figure 6b) during the first year of monitoring (i.e., from 23 January 2022 to 22 January 2023) – where the seasonal pattern on natural frequencies is highlighted: as temperature tends to increase towards hot season, all the natural frequencies decrease, and vice versa.

The variation in time of the natural frequencies of both bending and torsion modes and the correlation with temperature is exemplified in more details in figures 7 (mode B_1) and 8 (mode T_2): it should be noticed that the frequency-temperature correlation exhibits high coefficients of determination R^2 (0.739 for mode B_1 and 0.906 for mode T_2), clearly indicating that temperature turns out to be the dominant driver of frequency changes. It is also interesting to observe that the coefficients of determination between the frequencies identified in the first year of monitoring range between 0.53 and 0.98 (Table 1).

Table 2 summarizes the mean value (f_{mean}, ξ_{mean}) and the standard deviation (σ_f, σ_ξ) of the frequency and damping estimates as well as the mean and minimum value of the MAC and the identification rate.

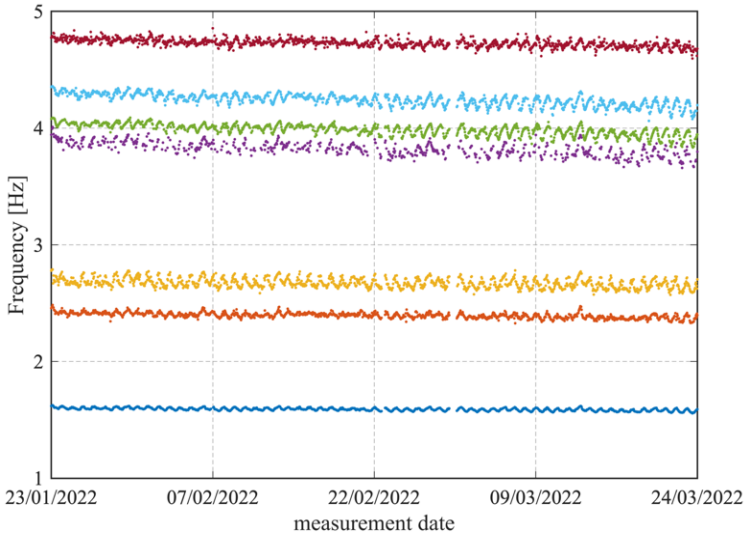

Figure 5. Identified natural frequencies from 23 January 2022 to 24 March 2022.

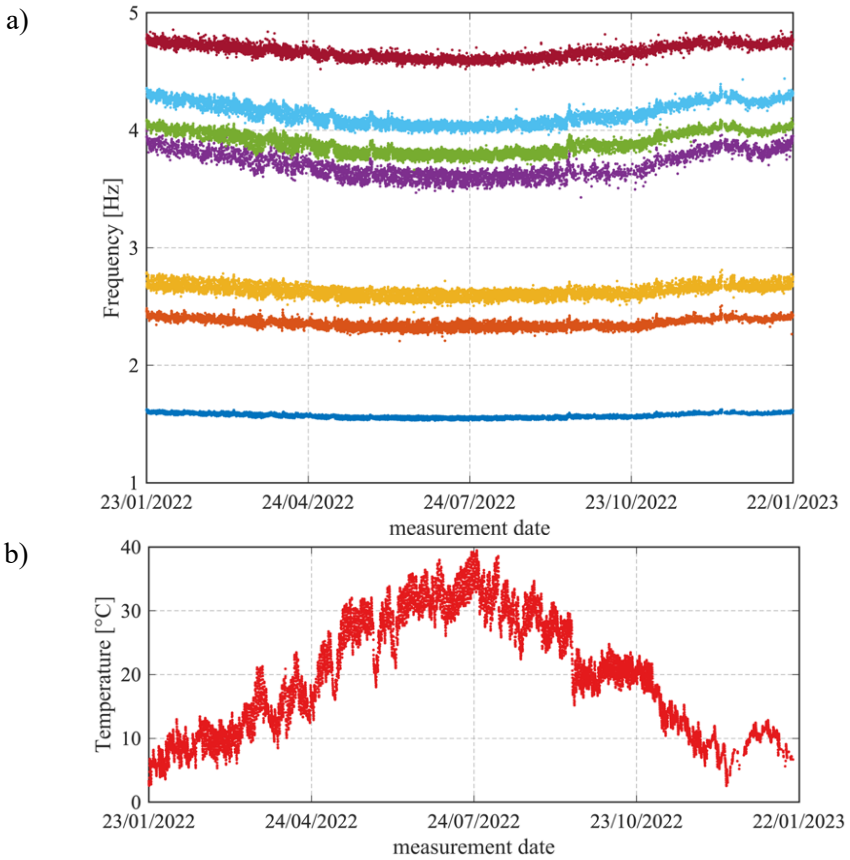

Figure 6. Identified natural frequencies (a) and measured temperature (b) from 23 January 2022 to 22 January 2023.

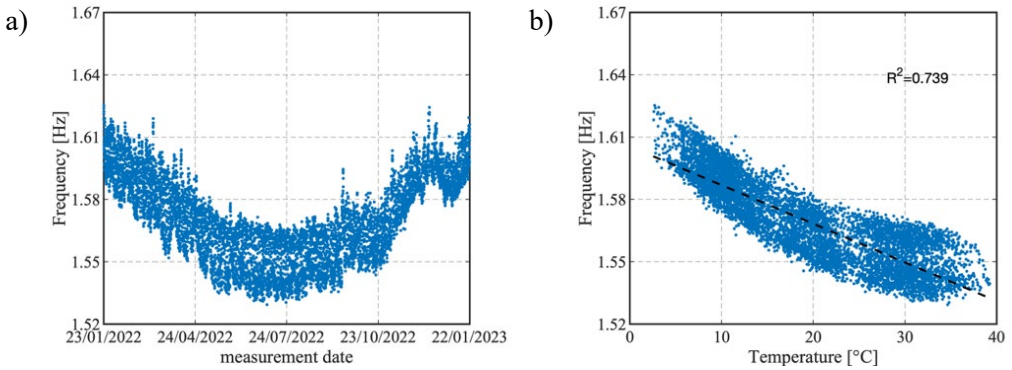

Figure 7. Mode B_1: evolution of natural frequency (a) and temperature-frequency correlation (b) from 23 January 2022 to 22 January 2023.

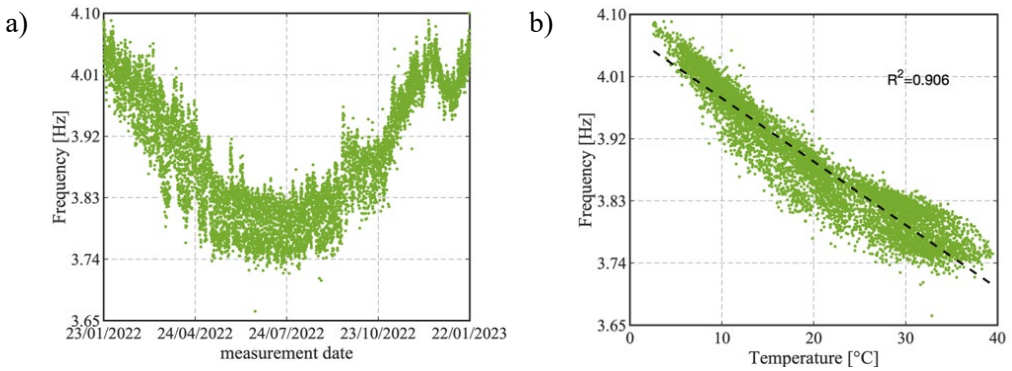

Figure 8. Mode T_2: evolution of natural frequency (a) and temperature-frequency correlation (b) from 23 January 2022 to 22 January 2023.

Table 1. Coefficients of determination R^2 between the natural frequencies identified from 23 January 2022 to 22 January 2023.

R^2	f_{B1}	f_{B2}	f_{B3}	f_{T1}	f_{T2}	f_{T3}	f_{B4}
f_{B1}	1	0.856	0.844	0.900	0.881	0.881	0.761
f_{B2}	–	1	0.767	0.763	0.722	0.735	0.631
f_{B3}	–	–	1	0.721	0.650	0.655	0.528
f_{T1}	–	–	–	1	0.923	0.926	0.865
f_{T2}	–	–	–	-	1	0.978	0.899
f_{T3}	–	–	–	-	-	1	0.905
f_{B4}	–	–	–	-	-	-	1

Although the inspection of figures 6-8 suggests that the time variation of natural frequencies is mostly arising from normal temperature changes, in order to assess the absence of any structural anomaly during the monitoring period, the effects of environmental and operational factors on identified frequencies have to be minimized/removed. To this purpose, a PCA model is defined assuming that the training period includes the first 8 months of monitoring (i.e., from 23 January 2022 to 22 October 2023). The frequency variation associated with the identified modes turns out to be explained by using two latent sources or variables; therefore, the first two PCs are retained in order to

establish the PCA-based model. Subsequently, the residuals between the identified and the predicted frequencies are computed, and a multi-variate T^2-Hotelling control chart [10] is constructed adopting an Upper Control Limit (UCL) set equal to the 95-th percentile of the residuals calculated during training period. The inspection of the control chart (figure 9) highlights the non-negligible occurrence of outliers between September and November 2022: those outliers are due to a temporary worsening of the signal-to-noise ratio in the collected signals. The increase in the noise of the measured accelerations, in turn, caused both a lower identification rate of some vibration modes (and the presence of outliers the T^2 control chart) and the decrease in the MAC values. On the other hand, the electrical malfunction was solved in the second part of November 2022 and the occurrence of outliers in figure 9 visibly vanishes, suggesting the absence of any appreciable structural anomalies in the first year of monitoring.

Table 2. Statistics of the modal parameters identified from 23 January 2022 to 22 January 2023.

Mode	f_{mean} (Hz)	σ_f (Hz)	ξ_{mean} (%)	σ_ξ (%)	MAC_{mean}	MAC_{min}	Id. Rate (%)
B_1	1.571	0.020	0.85	0.15	0.980	0.761	86.9
B_2	2.356	0.039	2.00	0.37	0.991	0.753	93.4
B_3	2.628	0.050	1.89	0.37	0.985	0.750	93.0
T_1	3.694	0.111	2.98	0.78	0.950	0.751	57.2
T_2	3.893	0.093	1.19	0.29	0.914	0.750	90.3
T_3	4.141	0.096	1.45	0.34	0.906	0.750	83.7
B_4	4.668	0.061	1.55	0.36	0.989	0.758	90.2

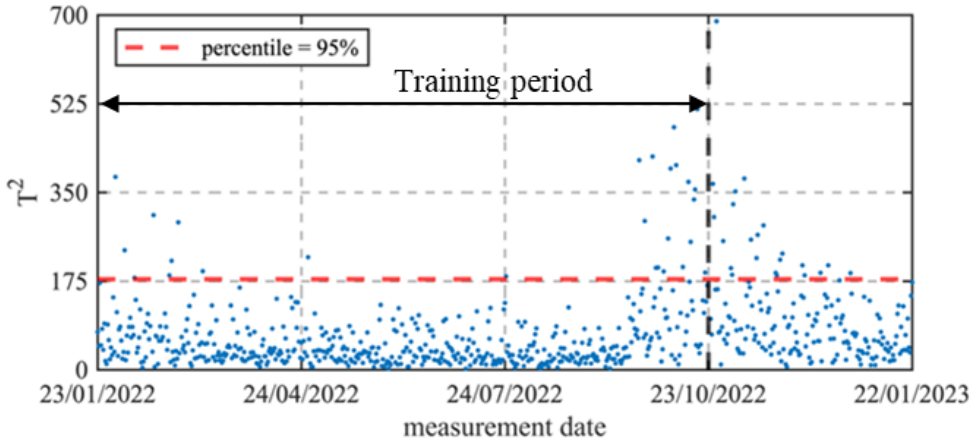

Figure 9. Hotelling-T^2 control-chart obtained from the residuals of frequencies (PCA).

Since the beginning of the monitoring period, the evolution of mode shapes is checked by means of the MAC (figures 10 and 11). Figure 10 refers to bending modes B_1-B_2 and does show appreciable MAC fluctuation or decrease only between September and November 2022 due to the previously mentioned increase of electrical noise in the monitoring system. The decrease of signal-to-noise ratio causes, in fact, higher MAC dispersion but after fixing the issue, the MACs returned close to unitary values.

Considering torsion modes (figure 11), instead, a visible seasonal pattern due to thermal variation is highlighted, which is a quite unusual behavior: in details, towards the hot season, the MAC value decreases. This phenomenon might be conceivably related to the elastic torsion supports (see figure 1a) constraints between the deck and the piers. Anyway, also for torsion modes, the MAC return to values in between 0.9 and 1.0 after hot season.

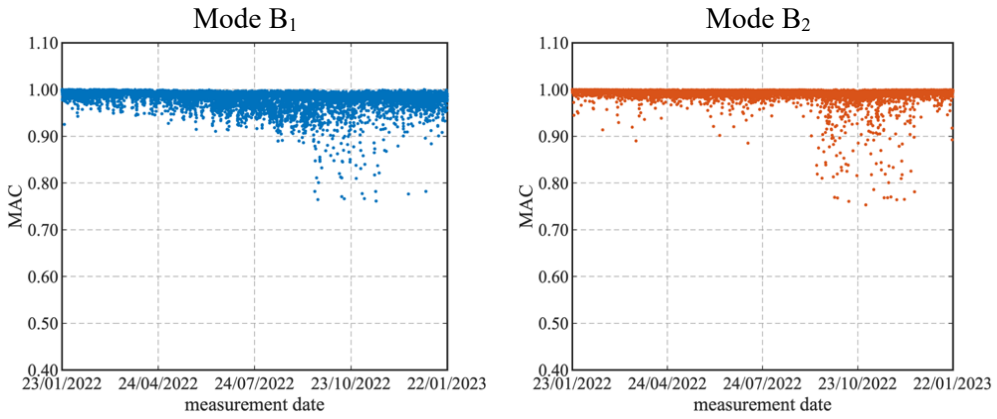

Figure 10. Typical evolution in time of MAC of bending modes B_1 and B_2.

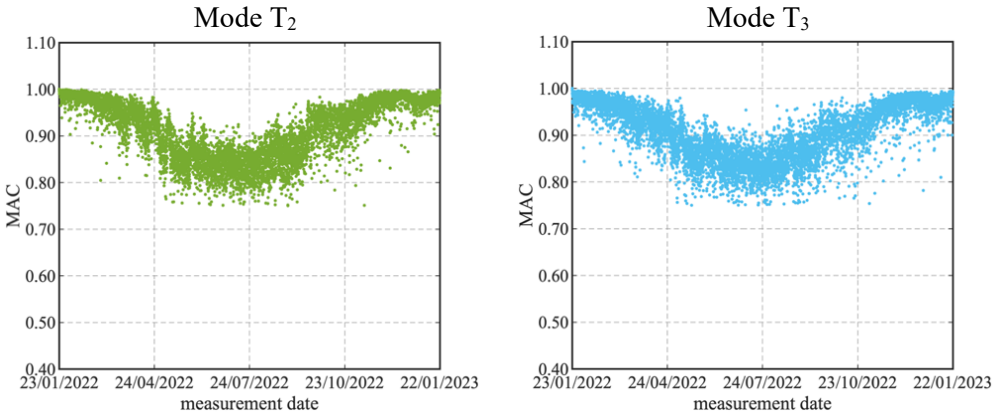

Figure 11. Typical evolution in time of MAC of bending modes T_2 and T_3.

5. Conclusions

The paper illustrates the OMA-based strategy adopted for the SHM of a steel-composite overpass. The main objective of the continuous dynamic monitoring is the evaluation of the effects of changing environments on the identified modal parameters and the detection of structural anomalies using both the cleansed natural frequencies and the changes in mode shapes.

Preliminary investigations and the first year of monitoring have shown the following results:

1. Seven vibration modes are identified in the frequency interval of 0-6 Hz and tracked by using software tools for the automated modal parameters estimation and tracking;
2. The air temperature turned out to be a dominant driver of the daily and seasonal fluctuation of the natural frequencies of all modes. In particular, the frequency values tend to decrease with increased temperature;
3. A PCA-based regression model, using two principal components, is used to minimize the environmental and operational effects on the natural frequencies. Subsequently, a T^2-Hotelling

control chart has not shown any structural change in the monitoring period. The structural condition preservation seems also confirmed by the MAC variation of the bending vibration modes, which tend to remain toward the unitary value.

4. By inspecting the MAC variation of the torsion modes, the effect of changing temperature is clearly detected, as the MAC values tend to decrease with increased temperature;
5. During a short period, an un-desired increase in the noise level of the collected signals has been detected in the T^2 control chart as well as through the dispersion in the MAC values of the bending modes.

Acknowledgments
The support of C.A.V. S.p.A. is gratefully acknowledged. Sincere thanks are due to M. Cucchi (VibLab, Laboratory of Vibrations and Dynamic Monitoring of Structures, Politecnico di Milano), who assisted the authors in conducting the field tests and to the technical staff of Nplus S.r.l. for the installation of the monitoring devices. The authors are indebted with M.Sc.Eng. Sabatino Fusco and M.Sc.Eng. Marco Scattolin for having allowed and encouraged the research.

References

[1] Federal Highway Administration 2008 *Status of the Nation's highways, bridges and transit: conditions and performance–Report to Congress* Technical Report, U S Department of Transportation
[2] Wenzel H 2009 *Health Monitoring of Bridges* (John Wiley & Sons)
[3] Peeters B and De Roeck G 2001 One-year monitoring of the Z24-bridge: environmental effects versus damage events *Earthq. Eng. Struct. D.* **30** pp 149-171
[4] Magalhães F, Cunha A and Caetano E 2012 Vibration based structural health monitoring of an arch bridge: from automated OMA to damage detection *Mech. Syst. Signal.* **28** pp 212-228
[5] Cross E J, Koo K Y, Brownjohn J M W and Worden K 2013 Long-term monitoring and data analysis of the Tamar Bridge *Mech. Syst. Signal Process*. **35(1-2)** pp 16-34
[6] Gentile C and Saisi A 2015 Continuous dynamic monitoring of a centenary iron bridge for structural modification assessment *Front. Struct. Civ. Eng*. **9** pp 26-41
[7] Borlenghi P, Gentile C and Pirrò M 2023 Continuous dynamic monitoring and automated Modal Identification of an arch bridge *European Workshop on Structural Health Monitoring*, ed P Rizzo and A Milazzo (Springer, Cham)
[8] Farrar C R and Worden K 2007 An introduction to structural health monitoring *Philos. Trans. R. Soc. Math. Phys. Eng. Sci.* **365(1851)** pp 303-315
[9] Sharma S 1995 *Applied Multivariate Techniques* (New York: John Wiley & Sons)
[10] Hotelling H 1947 *Multivariate quality control-illustrated by the air testing of sample bombsights* In eds C Eisenhart *et al* pp 111-184
[11] Pirrò M 2021 *Automated operational modal analysis and tracking: development of software tools and applications* (MSc Thesis) Politecnico di Milano, Italy
[12] Peeters B and De Roeck G 1999 Reference-based stochastic subspace identification for output-only modal analysis *Mech. Syst. Signal Process.* **13(6)** pp 855-878.
[13] Cabboi A, Magalhães F, Gentile C and Cunha À 2017 Automated modal identification and tracking: application to an iron arch bridge *Struct. Control Health Monit.* **24 (1)** pp e1854.
[14] Allemang R J and Brown D L 1982 A correlation coefficient for modal vector analysis *Proc. 1st Int. modal analysis Conf.*